Mon. Not. R. Astron. Soc. **361,** 511–516 (2005) doi:10.1111/j.1365-2966.2005.09171.x

Chandra observations of the millisecond X-ray pulsar IGR J00291+5934 in quiescence

P. G. Jonker,[1,2⋆] S. Campana,[3] D. Steeghs,[1] M. A. P. Torres,[1] D. K. Galloway,[4] C. B. Markwardt,[5,6] D. Chakrabarty[4] and J. Swank[5]

[1]*Harvard–Smithsonian Center for Astrophysics, 60 Garden Street, Cambridge, MA 02138, USA*
[2]*SRON, National Institute for Space Research, Sorbonnelaan 2, 3584 CA, Utrecht, the Netherlands*
[3]*INAF–Osservatorio Astronomico di Brera, Via Bianchi 46, I-23807 Merate (Lc), Italy*
[4]*Center for Space Research, Massachusetts Institute of Technology, Cambridge, MA 02139, USA*
[5]*Laboratory for High Energy Astrophysics, NASA, Goddard Space Flight Center, Greenbelt, MD 20771, USA*
[6]*Department of Astronomy, University of Maryland, College Park MD 20742, USA*

Accepted 2005 May 5. Received 2005 May 3; in original form 2005 February 9

ABSTRACT

In this paper we report on our analysis of three *Chandra* observations of the accretion-powered millisecond X-ray pulsar IGR J00291+5934 obtained during the late stages of the 2004 outburst. We also report the serendipitous detection of the source in quiescence by *ROSAT* during MJD 48830–48839 (1992 July 26–August 4). The detected 0.3–10 keV source count rates varied significantly between the *Chandra* observations from $(7.2 \pm 1.2) \times 10^{-3}$, $(6.8 \pm 0.9) \times 10^{-3}$ and $(1.4 \pm 0.1) \times 10^{-2}$ counts s^{-1} for the first, second and third *Chandra* observations, on MJD 53371.88 (2005 January 1), 53383.99 (2005 January 13) and 53407.57 (2005 February 6), respectively. The count rate for the third observation is 2.0 ± 0.4 times as high as that of the average of the first two observations. The unabsorbed 0.5–10 keV source fluxes for the best-fitting power-law model to the source spectrum were $(7.9 \pm 2.5) \times 10^{-14}$, $(7.3 \pm 2.0) \times 10^{-14}$, and $(1.17 \pm 0.22) \times 10^{-13}$ erg cm^{-2} s^{-1} for the first, second and third *Chandra* observations, respectively. We find that this source flux is consistent with that found by *ROSAT* [$\approx(5.4 \pm 2.4) \times 10^{-14}$ erg cm^{-2} s^{-1}]. Under the assumption that the interstellar extinction, $N_{\rm H}$, does not vary between the observations, we find that the blackbody temperature during the second *Chandra* observation is significantly higher than that during the first and third observations. Furthermore, the effective temperature of the neutron star derived from fitting an absorbed blackbody or neutron star atmosphere model to the data is rather high in comparison with many other neutron star soft X-ray transients in quiescence, even during the first and third observations. If we assume that the source quiescent luminosity is similar to that measured for two other accretion powered millisecond pulsars in quiescence, the distance to IGR J00291+5934 is 2.6–3.6 kpc.

Key words: accretion: accretion discs – binaries: general – stars: individual: IGR J00291+5934 – stars: neutron – X-rays: binaries.

1 INTRODUCTION

The evolutionary link between millisecond radio pulsars and low-mass X-ray binaries was established by the detection of the first accretion-powered millisecond X-ray pulsar SAX J1808.4–3658 (Wijnands & van der Klis 1998; Chakrabarty & Morgan 1998). Over the last few years, the number of known accretion-powered millisecond X-ray pulsars has steadily increased. Recently, the discovery of the sixth member of this class was announced. The source IGR J00291+5934 was discovered by the International Gamma-ray Astrophysics Laboratory (INTEGRAL; Eckert et al. 2004; Shaw et al. 2005) on 2004 December 2 (MJD 53341). Using *Rossi X-ray Timing Explorer* (*RXTE*) follow-up observations, Markwardt, Swank & Strohmayer (2004a) discovered pulsations at a frequency of 598.88 Hz. The pulsar is in a 147.4-min orbit with a low-mass companion star (Markwardt et al. 2004b; Galloway et al. 2005). A previously undetected source was found at a magnitude of $R \approx 17.4$ within the INTEGRAL error circle in an *R*-band image obtained with the Robotic Palomar 60-inch telescope (Fox & Kulkarni

⋆E-mail: pjonker@cfa.harvard.edu

2004). Spectra obtained with the 4.2-m William Herschel Telescope of this variable source showed Hα and He II emission lines, securing the identification of this variable star as the counterpart of IGR J00291+5934 (Roelofs et al. 2004; see also Filippenko, Foley & Callanan 2004). Finally, a variable radio and near-infrared source was found at the position of the optical counterpart (Fender et al. 2004; Pooley 2004; Steeghs et al. 2004).

During outburst, the X-ray, optical and radio properties of the accretion-powered X-ray pulsars are very similar to those of non-pulsating neutron star soft X-ray transients (SXTs; e.g. Wijnands & van der Klis 1999 for an X-ray account). In quiescence, the accretion powered X-ray pulsars observed so far with *Chandra* and/or *XMM–Newton* have lower luminosities than those of many non-pulsating neutron star SXTs in quiescence. Furthermore, in those quiescent systems where it has been possible to detect sufficient photons in X-rays to allow for a spectral decomposition, the X-ray spectrum is significantly harder than for the non-pulsating neutron star SXTs 4U 1608–52, Aql X–1, SAX J1748.8–2021 in the globular cluster NGC 6440, and XTE J1709-267 in quiescence (Asai et al. 1996; in't Zand et al. 2001; Campana et al. 2002; Rutledge et al. 2002a; Jonker et al. 2003; Cackett et al. 2005; Wijnands et al. 2005; see also Jonker et al. 2004b and references therein). However, there are systems that have intermediate spectral properties and luminosities (e.g. Jonker, Wijnands & van der Klis 2004a). Out of these sources with intermediate properties Cen X–4 (Rutledge et al. 2001), GRS 1741.9–2853 (Muno, Baganoff & Arabadjis 2003) and SAX J1810.8–2609 (Jonker et al. 2004a) have not been observed in outburst with the *RXTE* Proportional Counter Array. For this reason it is unclear whether pulsations were present in outburst or not.

The spectrum of several neutron star SXTs in quiescence is found to be well fit by a neutron star atmosphere (NSA) model sometimes supplemented with a power-law component. Especially in sources with a quiescent luminosity near 10^{33} erg s^{-1} the spectrum is dominated by a strong thermal component (Jonker et al. 2004b). Brown, Bildsten & Rutledge (1998) and Colpi et al. (2001) showed that the neutron star core is heated by pycnonuclear reactions during/immediately after accretion episodes. In quiescence, the heated neutron star core cools in X-rays. For a given core temperature, from the assumed thermal properties of the neutron star envelope, the cooling core spectral energy distribution is determined by the NSA. In theory, an NSA model fit to the quiescent thermal X-ray component provides the means to measure the mass and radius of the neutron star and hence constrain the equation of state of matter at supranuclear densities. In practice, numbers typical for a canonical neutron star were found (e.g. Heinke et al. 2003), rendering support for this interpretation. However, there is an ongoing debate about whether the temperature of the thermal component is varying or not (cf. Rutledge et al. 2002a; Campana & Stella 2003; Campana et al. 2004). Differences in temperatures obtained within one quiescent epoch may be explained by changes in the NSA due to ongoing low-level accretion (Brown, Bildsten & Chang 2002). Similarly, differences in the observed neutron star temperature obtained before and after outburst activity can be explained by differences in the amount of residual unburned light elements in the NSA (Brown et al. 2002). Large changes on short time-scales would render it unlikely that the soft/thermal component is due to cooling of the neutron star, limiting the applicability of the NSA model fit. Finally, there are currently two sources known (i.e. KS 1731–260 and MXB 1659–298) which returned to quiescence after an accretion epoch lasting several years. In these cases it is thought that the observed thermal spectral component is caused by the cooling of the neutron star crust (Rutledge et al. 2002b; Wijnands et al. 2002). The observed changes in the X-ray spectral properties are also ascribed to the cooling down of the neutron star crust (Wijnands et al. 2004).

In this paper we present the detailed analysis of three *Chandra* observations of the accretion powered X-ray pulsar IGR J00291+5934 obtained during the late stages of the 2004 outburst.

2 OBSERVATIONS, ANALYSIS AND RESULTS

We observed IGR J00291+5934 three times after the 2004 discovery outburst with the back-illuminated S3 CCD chip of the Advanced CCD Imaging Spectrometer (ACIS) detector on board the *Chandra* satellite. The observations started on MJD 53371.88 (2005 January 1; *Chandra* observation ID 6179), MJD 53383.99 (2005 January 13; observation ID 6180) and MJD 53407.57 (2005 February 6; observation ID 6181); all times are in UTC. The net, on-source exposure times were 4.7, 9.0 and 12.9 ks, respectively. We limited the readout area of the S3 chip to 1/8 of its original size yielding a smaller exposure time per CCD frame in order to avoid pile-up.

After the data were processed by the *Chandra* X-ray Center (ASCDS version 7.5.0), we analysed them using the CIAO 3.2.1 software developed by the *Chandra* X-ray Center. We searched the data for background flares but none was found; hence, we used all data in our analysis. We extracted data from a circular area with a radius of three pixels ($\sim$1.5 arcsec) centred on the best-fitting source position for the first two observations. This area encloses 90–95 per cent of the energy because, as we will show below, the source spectrum is not very hard. The reason why we use this small area is to exclude as much as possible background photons. In such a small area, one expects 1 ± 1 background photon for the first observation. During the third observation (MJD 53407.57) the count rate is higher than in the previous two observations (see below), which led us to use a six pixel ($\sim$3 arcsec) radius circular area centred on the source position for the source extraction.

In the three observations we detect, respectively, 36, 63 and 190 photons from a position consistent with that found in the optical by Fox & Kulkarni (2004) and in X-rays by Nowak et al. (2004). This yields 0.3–10 keV count rates of $(7.2 \pm 1.2) \times 10^{-3}$, $(6.8 \pm 0.9) \times 10^{-3}$ and $(1.4 \pm 0.1) \times 10^{-2}$ counts s^{-1}. These background-subtracted (see below) count rates are so low that pile-up is not a concern. The count rate for the third observation is 2.0 ± 0.4 times as high as that of the average of the first two observations. Due to the low number of source counts, the Cash statistic was used for the spectral analysis of the first two observations (Cash 1979). This means that the background should not be subtracted when fitting the spectrum in order to maintain the counting statistics (although with a background as low as this in our case, this should not make much difference). For the extraction of the background spectrum in the third observation, we used an annulus with radius of 5–15 arcsec. We rebinned the source spectrum of the third observation such that each bin contains at least 10 counts. We fitted the spectra in the 0.3–10 keV range using XSPEC (Arnaud 1996) version 11.3.1. Because 10 counts per bin is still low for the use of χ^2 statistics in the spectral fits of the third observation, we compared the results using the χ^2 statistics with those obtained using the Cash statistics; the results are the same within the errors.

For each observation separately we searched for variability in the light curve. Only in the last observation (ID 6181) is there evidence that the source count rate was higher towards the end of the observation than near the start of the observation (see Fig. 1). A Kolmogorov–Smirnov test (see Press et al. 1992), testing the hypothesis that the count rate of the source is constant, showed that the probability that the count rate is constant is 0.36, 0.36 and

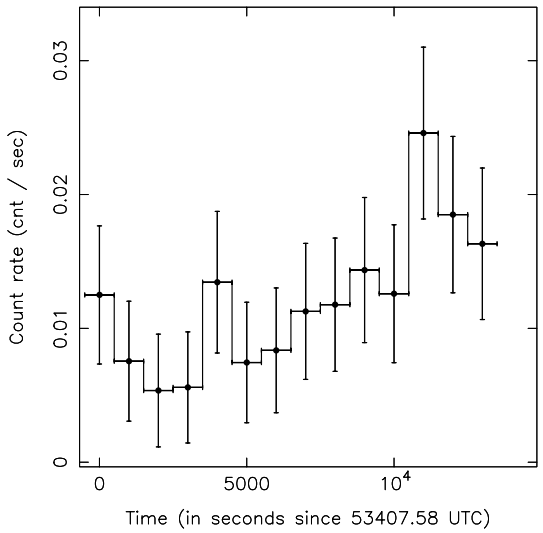

Figure 1. The 0.3–10 keV background-subtracted light curve for the accretion-powered millisecond X-ray pulsar IGR J00291+5934 detected with the *Chandra* satellite on MJD 53407.57. The data were binned in 1000-s intervals. Variability in the count rate as a function of time within the observation is clearly detected.

8.4×10^{-5} for observations with ID 6179, 6180 and 6181, respectively (i.e. the hypothesis is observed to be disproven at the 4.1σ level for the third observation). We searched for spectral variability within an observation by making hardness ratios for the first and second halves of the total number of photons detected during each observation and by investigating the photon energy as a function of photon arrival time. The hardness is defined as the count rate ratio between the 0.3–1.5 and 1.5–10 keV bands. There is no evidence for significant changes in the hardness ratio during any of the observations. To check whether the hardness ratio changes between the observations, we calculated the hardness ratio from all photons detected during one observation. The hardness ratio during the first, second and third observations is 2.8 ± 1.1, 1.3 ± 0.3, and 2.3 ± 0.4, respectively. The hardness ratio of the third observation is larger than that of the second observation, albeit at the 2σ level.

In order to check whether the spectrum changed between the observations, we fitted the spectra for each of the observations separately. We fit the spectra using several functions that are often used for quiescent neutron stars (a power law, an NSA and a blackbody model), all of which were modified by the effects of interstellar absorption. In these fits, the value of the interstellar absorption, $N_{\rm H}$, was fixed to 2.8×10^{21} cm^{-2} similar to the value found by Nowak et al. (2004). When we left $N_{\rm H}$ as a free parameter in the spectral fits for the third observation, $N_{\rm H}$ was consistent with 2.8×10^{21} cm^{-2}. As an indication of the influence that fixing $N_{\rm H}$ has on the fit parameters, we include the results of a blackbody, a power law and a blackbody fit to the first, second and third observation, respectively, in Table 1. For the NSA model, the neutron star radius and mass are fixed to 10 km and 1.4 $M_\odot$, respectively. Furthermore, we have assumed that the neutron star magnetic field is so low that it is unimportant for the NSA modelling, leaving only the normalization (i.e. one divided by the source distance squared) and the effective temperature as free parameters in this model. The results of these fits are shown in Table 1.

The likelihood ratio method, which is the basis of the Cash statistic, does not provide a direct test to the goodness of fit, which would help one to distinguish between different models (e.g. Bevington

Table 1. Best-fitting parameters of the quiescent spectrum of IGR J00291+5934. NSA stands for neutron star atmosphere, BB refers to blackbody, and PL to power law. All quoted errors are at the 90 per cent confidence level. The value in brackets in the flux column denotes the (95 per cent upper limit to the) fractional contribution of a PL in the case of a BB or NSA model fit or a BB/NSA in the case of a PL model fit. In the case of an upper limit to the fractional PL contribution, the PL index was fixed at 2. In the case of an upper limit to the fractional BB/NSA contribution, the BB/NSA temperature was fixed at 0.2 keV/10^6 K. For the first two observations, the goodness of fit is expressed via the goodness parameter, whereas for the third observation the goodness of fit is given by means of the reduced χ^2 for a certain degrees of freedom (d.o.f.).

Obs ID	MJD (UTC)	Model	$N_{\rm H} \times 10^{21}$ cm^{-2}	BB radius (d/10 kpc)^2 km	NSA norm. (10 kpc/d)^2	PL norm. $\times 10^{-5}$ phot. keV^{-1} cm^{-2} s^{-1}	Temp./PL index BB (keV), NSA (log K)	Unabs. 0.5–10 keV flux (erg cm^{-2} s^{-1})	Goodness/$\chi^2_{\rm red}$ per cent/d.o.f.
6179	53371.88	BB	2.8[a]	$1.1^{+1.9}_{-0.7}$	–	–	0.27 ± 0.05	5.2×10^{-14} (<43 per cent[b])	6 per cent
6179	53371.88	NSA	2.8[a]	–	$0.21^{+1.01}_{-0.17}$	–	6.25 ± 0.15	5.5×10^{-14} (<39 per cent[b])	34 per cent
6179	53371.88	PL	2.8[a]	–	–	2.6 ± 0.8	3.2 ± 0.7	7.9×10^{-14} (<23/26 per cent[b])	3 per cent
6179	53371.88	BB	$0.8^{+3}_{-0.8}$	$0.36^{+3.6}_{-0.26}$	–	–	0.32 ± 0.10	3.5×10^{-14} (<47 per cent[b])	31 per cent
6180	53383.99	BB	2.8[a]	$(5.8^{+4.6}_{-2.7}) \times 10^{-2}$	–	–	0.54 ± 0.09	5.3×10^{-14} (<68 per cent[b])	99 per cent
6180	53383.99	NSA	2.8[a]	–	$(0.40^{+0.46}_{-0.27}) \times 10^{-2}$	–	6.65 ± 0.10	5.7×10^{-14} (<53 per cent[b])	88 per cent
6180	53383.99	PL	2.8[a]	–	–	1.8 ± 0.5	2.3 ± 0.4	7.3×10^{-14} (<15/18 per cent[b])	14 per cent
6180	53383.99	PL	$0.7^{+2.4}_{-0.7}$	–	–	$1.0^{+1.0}_{-0.4}$	1.7 ± 0.6	6.3×10^{-14} (<10/10 per cent[b])	24 per cent
6181	53407.57	BB	2.8[a]	1.0 ± 0.5	–	–	0.31 ± 0.03	8.3×10^{-14} (<27 per cent[b])	1.0/13
6181	53407.57	NSA	2.8[a]	–	$0.15^{+0.14}_{-0.1}$	–	$6.33^{+0.11}_{-0.06}$	9.0×10^{-14} (<25 per cent[b])	0.96/13
6181	53407.57	PL	2.8[a]	–	–	4.1 ± 0.6	2.9 ± 0.3	1.3×10^{-13} (<12/12 per cent[b])	1.4/13
6181	53407.57	BB+PL	2.8[a]	1.16 ± 0.57	–	$0.7^{+15}_{-0.7}$	$0.28 \pm 0.05/2^a$	1.0×10^{-13} ($67 + 33$ per cent[b])	1.0/12
6181	53407.57	BB	$1.3^{+2.7}_{-1.3}$	$0.48^{+1.5}_{-0.3}$	–	–	0.34 ± 0.07	6.5×10^{-14} (<25 per cent[b])	1.0/12

Notes. [a]Parameter fixed. [b]Percentage contributed to the total flux/upper limit to the fractional BB/NSA or PL contribution to the total flux.

& Robinson 1992). In order to obtain a handle on the goodness of fit, we used Monte Carlo simulations. They consist of simulating 10^4 counts spectra. Each spectrum is drawn from a parent distribution with Poisson statistics. The parent distribution is allowed to vary according to the covariances of the best-fitting model parameters. The C fit-statistic for each of the Monte Carlo simulations is compared with that of the best-fitting model. After the Monte Carlo simulations have been performed, the fraction of simulations that gave a lower fit statistic than that of the best-fitting model is given. This percentage is called the 'goodness'. If the model provides a good description of the data, the goodness should be close to 50 per cent. Both a very low goodness and a very high goodness indicate that the model does not represent the data accurately. As can be seen in Table 1, for many of the single-component models for which $N_{\rm H}$ was held fixed at 2.8×10^{21} cm^{-2}, the goodness is not close to the nominal 50 per cent. However, in none of the cases can we exclude the model at high significance based on the goodness.

The spectral fits suggest that the spectrum of the source is harder during the second observation than during the first and third observations, as can be seen from a comparison between the best-fitting power-law index or the blackbody/NSA temperature of the observations. Besides the single-component models, we tried fitting a model comprised of a blackbody and a power law modified by the effects of interstellar absorption to the data in order to assess the contribution of a power law to the spectrum. However, due to the low number of detected photons during the first and second observations, the fit parameters were unconstrained. A fit using such a fit function resulted in meaningful constraints only for the third observation (and only when we kept the power-law index fixed to 2). The results of this fit are also listed in Table 1. We also tried to fit an NSA plus power-law model to the spectrum of the third observation. However, with the power-law index fixed to a value of 2, the power law did not contribute significantly to the fit (the normalization was a factor of 10^3 less than that found for the blackbody plus power-law fit). In Fig. 2 we have plotted the spectrum showing a power-law fit to the data set of the second *Chandra* observation and a blackbody fit to the third *Chandra* observation.

The unabsorbed 0.5–10 keV source flux for the first, second and third *Chandra* observations using the best-fitting power-law model is $(7.9 \pm 2.5) \times 10^{-14}$, $(7.3 \pm 2.0) \times 10^{-14}$ and $(1.17 \pm 0.22) \times 10^{-13}$ erg cm^{-2} s^{-1}, respectively (see Fig. 3; the plotted uncertainty on these fluxes is at the 68 per cent confidence level). We also listed in Table 1 the unabsorbed 0.5–10 keV flux for each model for each observation. In between brackets we give the upper limit to the fractional contribution to the unabsorbed 0.5–10 keV flux for a power-law model in the case of a blackbody or NSA model fit. We also give the upper limit to the fractional contribution for a blackbody and NSA model in the case of a power-law fit.

Finally, we extracted an 18-ks archival Positional Sensitive Proportional Counter (PSPC) *ROSAT* observation of the cataclysmic variable RX J0028.8+5917, also known as DQ Her, obtained over the period MJD 48830–48839 (1992 July 26–August 4). Besides DQ Her, a source is detected at a position consistent within the *ROSAT* PSPC positional accuracy with that of IGR J00291+5934. There are 44 counts in a circular region with radius of 40 arcsec in the 0.1–2 keV energy range. However, from a background determination of a circular region 100 arcsec away, we find that 43 per cent of those counts can be attributed to the background. This yields a background-subtracted source count rate of $(1.4 \pm 0.4) \times 10^{-3}$ counts s^{-1} in the PSPC instrument. If we use a power law with index 2.5 and fix $N_{\rm H}$ to 2.8×10^{21} cm^{-2}, we obtain an unabsorbed 0.5–10 keV source flux of $\approx(5.4 \pm 2.4) \times 10^{-14}$ erg cm^{-2} s^{-1} at the time of the *ROSAT* observation.

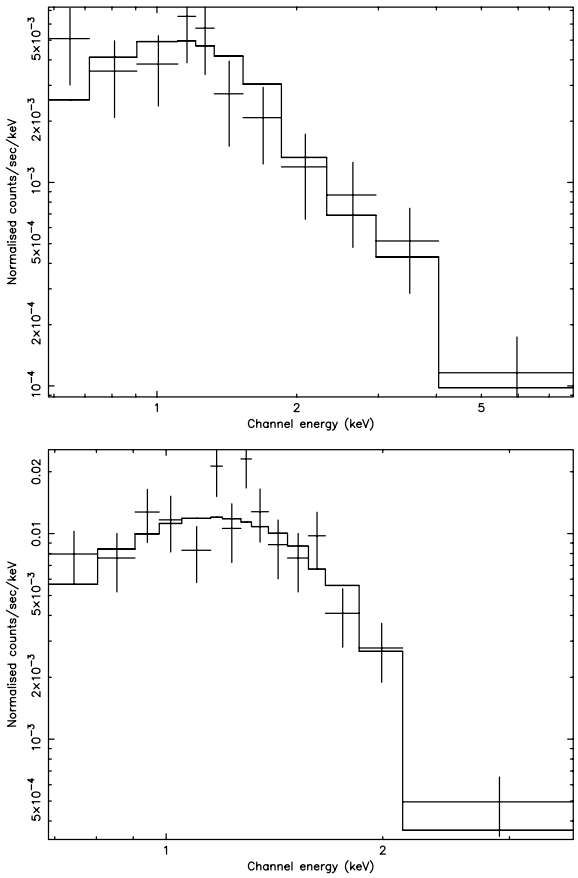

Figure 2. Top panel: the quiescent spectrum of IGR J00291+5934 detected with the *Chandra* satellite on MJD 53383.99 (2005 January 13). The best-fitting power-law model is overplotted. The fit was performed on the unbinned data using the C-statistic, but for clarity the data points have been rebinned in the plot. Bottom panel: the quiescent spectrum of IGR J00291+5934 detected with the *Chandra* satellite on MJD 53407.57 (2005 February 6). The best-fitting blackbody model is overplotted. In both cases, $N_{\rm H}$ was fixed to 2.8×10^{21} cm^{-2}.

3 DISCUSSION

We have presented the analysis of three *Chandra* observations of the accretion-powered millisecond X-ray pulsar IGR J00291+5934. The observations were obtained right after the end of the 2004 discovery outburst. The count rate for the third observation is 2.0 ± 0.4 times higher than that of the average of the first two observations. This shows that even in quiescence, there is evidence for variability (at the $\sim 5\sigma$ level). However, owing to spectral variability between the three observations, the unabsorbed 0.5–10 keV source flux of the *Chandra* observations did not change significantly. We also detected the source in quiescence in a *ROSAT* observation obtained in 1992. The flux that we measured in the *Chandra* observations does not differ significantly from that in the 1992 *ROSAT* observation. From this we derive that the source had reached quiescence already during our first *Chandra* observation obtained $\sim$31 d after the discovery of the source (Shaw et al. 2005).

Under the assumption that the interstellar extinction, $N_{\rm H}$, does not vary between the observations, we find from a blackbody/NSA fit

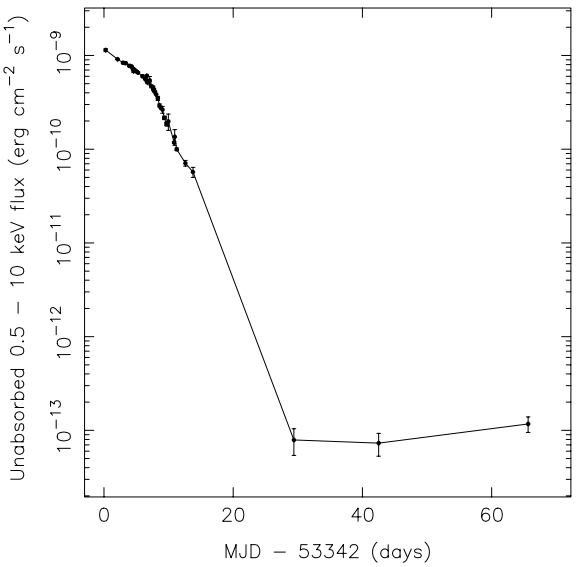

Figure 3. The 0.5–10 keV unabsorbed 2004/2005 outburst light curve for the accretion-powered millisecond X-ray pulsar IGR J00291+5934 as detected with the *RXTE* and *Chandra* satellites. The *RXTE* 2.5–25 keV observed flux (Galloway et al. 2005) is converted to an unabsorbed 0.5–10 keV flux using a power-law spectrum with index 2 and an interstellar absorption of $N_{\rm H} = 2.8 \times 10^{21}$ cm^{-2}.

to the spectrum of the second observation that the blackbody/NSA temperature is significantly higher than that during the first and third observations. Furthermore, a single model fit using either an NSA or a blackbody model with $N_{\rm H}$ fixed to the value derived during outburst ($N_{\rm H} = 2.8 \times 10^{21}$ cm^{-2}; Nowak et al. 2004) yields a rather high temperature when compared with other neutron star SXTs in quiescence even for the first and third observations; cf. $T_{\rm BlackBody} = 0.27 \pm 0.05$, 0.31 ± 0.03 keV/$\log(T_{\rm NSA}) = 6.25 \pm 0.15$, $6.33^{+0.11}_{-0.06}$ for the first and third observations of IGR J00291+5934, respectively, whereas $\log(T_{\rm NSA}) = 5.84$–6.14 for Aql X-1 (range due to variability; Rutledge et al. 2002a), $T_{\rm BlackBody} = 0.186 \pm 0.005$ keV/$\log(T_{\rm NSA}) = 5.99 \pm 0.02$ for Cen X-4 (Campana et al. 2004), $T_{\rm BlackBody} = 0.14 \pm 0.02$ keV for SAX J1810.8–2609 (Jonker et al. 2004a), $T_{\rm BlackBody} = 0.24 \pm 0.02$ keV for XTE J1709–267 (Jonker et al. 2004b), and $\log(T_{\rm NSA}) = 6.02$–6.24 for SAX J1748.8–2021 in the globular cluster NGC 6440 (range due to variability; Cackett et al. 2005). Even when we leave $N_{\rm H}$ as a free parameter, the best-fitting blackbody temperature is 0.32 ± 0.06 keV for the third observation. Such a high temperature can be explained if the source spectrum contains a harder component besides a single (absorbed) thermal component. For the last and longest observation, the signal-to-noise ratio is high enough to test this by fitting the data with a model consisting of a blackbody and a power law, modified by the effects of interstellar absorption. This provides a good fit with a slightly lower blackbody temperature of 0.28 ± 0.05 keV when we fix the power-law index to 2. In this case, the power law contributes 33 per cent to the source luminosity.

Rutledge et al. (2002a) and Campana et al. (2004) showed that the quiescent spectra and flux of Aql X-1 and Cen X-4 also vary during and between observations. However, in their interpretation these authors differ. Campana & Stella (2003) showed that with the current data for Aql X-1, it is not possible to distinguish between intrinsic source variability in the soft blackbody component and correlated variability in the interstellar column density and the power-law photon index. Here we show, for the first time, that besides in these two canonical neutron star SXTs, spectral and count rate variability also occurs in the quiescent X-ray emission of an accretion-powered millisecond X-ray pulsar. Significant variability in the light curve was also found during the last observation. At the 95 per cent confidence level, there is evidence for variability during an observation of the accretion-powered millisecond X-ray pulsar XTE J0929–314 (Wijnands et al. 2005). As explained in Section 1, the variability observed in the quiescent flux of the neutron star SXTs KS 1731–260 and MXB 1659–29 (Wijnands et al. 2002, 2004) likely has a different origin than the variability observed here. Similarly, the variability of SAX J1748.8–2021 in the globular cluster NGC 6440 in quiescence (Cackett et al. 2005) can be caused by the fact that in between the two quiescent observations the source experienced an outburst. The quiescent flux of GRS 1741.9–2853 was found to vary by more than a factor of 5 (Muno et al. 2003). However, this source has, so far, never been observed in outburst with *RXTE*, and hence it is unclear whether this source contains an accretion-powered millisecond X-ray pulsar.

The ratio between the peak and lowest quiescent unabsorbed 0.5–10 keV X-ray flux is $\sim 2 \times 10^4$. This was found after correcting the peak flux given in Galloway et al. (2005) for the different bandpass assuming the peak-flux spectrum is similar to the spectrum found by Nowak et al. (2004). This ratio is low for an SXT. Unfortunately, the distance to IGR J00291+5934 is not well constrained, so in principle we cannot say whether the quiescent luminosity is high or the outburst luminosity is low (or both). Galloway et al. (2005) mention a minimum distance of 4 kpc, but as these authors also state, the uncertainty in this estimate is large. If we assume that IGR J00291+5934 has a 0.5–10 keV quiescent luminosity of ≈ 5–10×10^{31} erg s^{-1}, similar to that of the accretion-powered millisecond pulsars SAX J1808.4-3658 and XTE J0929–314 (Campana et al. 2002; Wijnands et al. 2005), the distance to IGR J00291+5934 would be $\approx$2.6–3.6 kpc. In light of the uncertainty of this estimate, the values derived by us and Galloway et al. (2005) are close together. However, an NSA model does not provide a satisfactory fit to the spectrum of our third *Chandra* observation if we fix the model normalization to that obtained for a distance of 3.5 kpc ($\chi^2_{\rm red} = 3.7$ for 14 degrees of freedom). If we let $N_{\rm H}$ free the $\chi^2_{\rm red} = 1.5$ for 13 degrees of freedom with $N_{\rm H} = 0.65^{+0.28}_{-0.08} \times 10^{21}$ cm^{-2} for an NSA temperature of 94 ± 4 eV.

Because this source is relatively bright in X-rays in quiescence, a future, longer *XMM–Newton* or *Chandra* observation should provide better constraints on the spectral parameters and test for the time-scale of variability.

ACKNOWLEDGMENTS

PGJ would like to thank the *Chandra* Director, Harvey Tananbaum, for the allocation of Director's Discretionary Time and the *Chandra* support team for help with preparing the observations and the fast processing of the data. The authors would like to thank the referee for useful comments and suggestions, which helped improve the paper, and Mariano Méndez for reading and commenting on an earlier version of the manuscript. Support for this work was provided by the National Aeronautics and Space Administration (NASA) through *Chandra* Postdoctoral Fellowship grant number PF3–40027 awarded by the *Chandra* X-ray Center, which is operated by the Smithsonian Astrophysical Observatory for NASA under contract NAS8–39073. DS acknowledges a Smithsonian Astrophysical Observatory Clay Fellowship. PGJ further acknowledges support from NASA grant GO4-5033X Fund number 16617404.

REFERENCES

Arnaud K. A., 1996, in Jacoby G. H., Barnes J., eds, ASP Conf. Ser. Vol. 101, Astronomical Data Analysis Software and Systems V. Astron. Soc. Pac., San Francisco, p. 17

Asai K., Dotani T., Mitsuda K., Hoshi R., Vaughan B., Tanaka Y., Inoue H., 1996, PASJ, 48, 257

Bevington P. R., Robinson D. K., 1992, Data Reduction and Error Analysis for the Physical Sciences, 2nd edn. McGraw-Hill, New York

Brown E. F., Bildsten L., Rutledge R. E., 1998, ApJ, 504, L95

Brown E. F., Bildsten L., Chang P., 2002, ApJ, 574, 920

Cackett E. M. et al., 2005, ApJ, 620, 922

Campana S., Stella L., 2003, ApJ, 597, 474

Campana S. et al., 2002, ApJ, 575, L15

Campana S., Israel G. L., Stella L., Gastaldello F., Mereghetti S., 2004, ApJ, 601, 474

Cash W., 1979, ApJ, 228, 939

Chakrabarty D., Morgan E. H., 1998, Nat, 394, 346

Colpi M., Geppert U., Page D., Possenti A., 2001, ApJ, 548, L175

Eckert D., Walter R., Kretschmar P., Mas-Hesse M., Palumbo G. G. C., Roques J.-P., Ubertini P., Winkler C., 2004, The Astronomer's Telegram, 352, 1

Fender R., De Bruyn G., Pooley G., Stappers B., 2004, The Astronomer's Telegram, 361, 1

Filippenko A. V., Foley R. J., Callanan P. J., 2004, The Astronomer's Telegram, 366, 1

Fox D. B., Kulkarni S. R., 2004, The Astronomer's Telegram, 354, 1

Galloway D. K., Markwardt C. B., Morgan E. H., Chakrabarty D., Strohmayer T. E., 2005, ApJ, 622, L45

Heinke C. O., Grindlay J. E., Lugger P. M., Cohn H. N., Edmonds P. D., Lloyd D. A., Cool A. M., 2003, ApJ, 598, 501

in't Zand J. J. M., van Kerkwijk M. H., Pooley D., Verbunt F., Wijnands R., Lewin W. H. G., 2001, ApJ, 563, L41

Jonker P. G., Méndez M., Nelemans G., Wijnands R., van der Klis M., 2003, MNRAS, 341, 823

Jonker P. G., Wijnands R., van der Klis M., 2004a, MNRAS, 349, 94

Jonker P. G., Galloway D. K., McClintock J. E., Buxton M., Garcia M., Murray S., 2004b, MNRAS, 354, 666

Markwardt C. B., Swank J. H., Strohmayer T. E., 2004a, The Astronomer's Telegram, 353, 1

Markwardt C. B., Galloway D. K., Chakrabarty D., Morgan E. H., Strohmayer T. E., 2004b, The Astronomer's Telegram, 360, 1

Muno M. P., Baganoff F. K., Arabadjis J. S., 2003, ApJ, 598, 474

Nowak M. A. et al., 2004, The Astronomer's Telegram, 369, 1

Pooley G., 2004, The Astronomer's Telegram, 355, 1

Press W. H., Teukolsky S. A., Vetterling W. T., Flannery B. P., 1992, Numerical Recipes in FORTRAN. The Art of Scientific Computing, 2nd edn. Cambridge Univ. Press, Cambridge

Roelofs G., Jonker P. G., Steeghs D., Torres M., Nelemans G., 2004, The Astronomer's Telegram, 356, 1

Rutledge R. E., Bildsten L., Brown E. F., Pavlov G. G., Zavlin V. E., 2001, ApJ, 551, 921

Rutledge R. E., Bildsten L., Brown E. F., Pavlov G. G., Zavlin V. E., 2002a, ApJ, 577, 346

Rutledge R. E., Bildsten L., Brown E. F., Pavlov G. G., Zavlin V. E., Ushomirsky G., 2002b, ApJ, 580, 413

Shaw S. E. et al., 2005, A&A, 432, L13

Steeghs D., Blake C., Bloom J. S., Torres M. A. P., Jonker P. G., Starr D., 2004, The Astronomer's Telegram, 363, 1

Wijnands R., van der Klis M., 1998, Nat, 394, 344

Wijnands R., van der Klis M., 1999, ApJ, 514, 939

Wijnands R., Guainazzi M., van der Klis M., Méndez M., 2002, ApJ, 573, L45

Wijnands R., Homan J., Miller J. M., Lewin W. H. G., 2004, ApJ, 606, L61

Wijnands R., Homan J., Heinke C. O., Miller J. M., Lewin W. H. G., 2005, ApJ, 619, 492

This paper has been typeset from a TEX/LATEX file prepared by the author.